Journal of Dental Sciences 21 (2026) 206–215

Available online at www.sciencedirect.com

ScienceDirect

journal homepage: www.e-jds.com

Original Article

Ferritin promotes monocyte osteoclastogenic differentiation to aggravate alveolar bone resorption in periodontitis

Wenxue Huang [a†], Jie Zhang [b†], Menglong Hu [c†], Zhaoguo Yue [b], Ye Han [b], Xiaochi Chang [b], Jianxia Hou [b*]

[a] *Department of Stomatology, Beijing Shijitan Hospital, Capital Medical University, Beijing, China*
[b] *Department of Periodontology, Peking University School and Hospital of Stomatology, Beijing, China*
[c] *Department of Prosthodontics, Peking University School and Hospital of Stomatology, Beijing, China*

Received 17 May 2025; Final revision received 29 May 2025
Available online 11 June 2025

KEYWORDS
Ferritin;
Periodontitis;
Osteoclastogenesis;
Alveolar bone resorption;
Monocytes

Abstract *Background/purpose:* Alveolar bone resorption in periodontitis critically impairs masticatory function and tooth stability, yet the mechanistic drivers linking immune dysregulation to osteolytic pathology remain incompletely characterized. This study elucidates how ferritin-an inflammation responsive iron chaperone secreted by activated monocytes-orchestrates monocyte-to-osteoclast differentiation to exacerbate bone destruction in periodontitis.

Materials and methods: Using a multidisciplinary approach, we combined: Immunohistochemical profiling of cluster of differentiation 68-positive ($CD68^+$) cells and cluster of differentiation 4-positive ($CD4^+$) cells in human periodontal tissues (periodontitis vs. healthy controls); Murine experimental periodontitis induced by maxillary molar ligation (8-week model); *In vitro* mechanistic studies where THP-1 monocytes (human acute monocytic leukemia cell line) primed with *Porphyromonas gingivalis* lipopolysaccharide (*P. gingivalis*-LPS) were analyzed for ferritin/receptor activator of nuclear factor-κB ligand (RANKL) secretion, and RAW264.7 pre-osteoclasts (murine macrophage-like cell line) were treated with apoferritin ± RANKL to assess proliferation, osteoclast differentiation, and osteolytic gene expression.

Results: Inflamed periodontal tissues exhibited elevated $CD68^+$ and $CD4^+$ immune cells, reflecting heightened inflammatory activity. *P. gingivalis*-LPS stimulation increased ferritin and RANKL secretion in THP-1 cells. Mice with experimental periodontitis showed increased osteoclast density at alveolar bone surfaces. Apoferritin synergized with RANKL to enhance RAW264.7 proliferation, multinucleation, and expression of matrix metallopeptidase 9 (MMP-

* Corresponding author. No. 22, Zhongguancun South Avenue, Haidian District, Beijing 100081, China.
E-mail address: jxhou@163.com (J. Hou).
† Wenxue Huang, Jie Zhang and Menglong Hu contributed equally to this work.

https://doi.org/10.1016/j.jds.2025.05.034

9), cathepsin K (CTSK), and tartrate-resistant acid phosphatase (TRAP) in a dose-dependent manner.
Conclusion: Ferritin and RANKL synergistically promote monocyte osteoclastogenesis, driving alveolar bone resorption in periodontitis. Targeting ferritin signaling may offer therapeutic potential to mitigate bone loss.

Introduction

Periodontitis, a chronic inflammatory disease affecting over 50 % of adults worldwide, represents the primary cause of tooth loss through its characteristic progressive alveolar bone destruction.[1,2] While microbial dysbiosis initiates periodontal inflammation, emerging evidence underscores that maladaptive host immune responses-particularly monocyte/macrophage hyperactivity-constitute the critical driver of osteolytic pathology.[3—5] Despite advances in biofilm control strategies, many patients exhibit refractory bone loss, highlighting our incomplete understanding of the molecular mechanisms governing osteoclast hyperactivity.[6] This knowledge gap urgently demands identification of novel therapeutic targets within the immune—osteoclast axis.

Our clinical observations reveal a striking correlation between circulating monocyte levels and radiographic bone loss severity. These circulating precursors, upon infiltrating periodontal tissues through C—C motif chemokine ligand 2 (CCL2)-mediated chemotaxis,[7] undergo pathological differentiation into bone-resorbing osteoclasts-multinucleated TRAP $^{+}$ cells capable of degrading a mass of mineralized matrix daily.[8,9]

Monocytes and macrophages infiltrate inflamed periodontal tissues, differentiating into osteoclasts under inflammatory cues.[10] Notably, the inflammatory milieu of infrabony pockets creates a self-perpetuating niche: immune cells form cellular networks within granulation tissue, while periodontal pathogens like *Porphyromonas gingivalis* (*P. gingivalis*) release virulence factors that hijack iron metabolism pathways.[11]

Central to this process is ferritin, the iron-sequestering protein paradoxically elevated in periodontal inflammations.[12,13] Our preliminary work demonstrated that *P. gingivalis* -derived lipopolysaccharide (LPS) promote the expression and secretion of ferritin in periodontal ligament cells.[14] Building on the established synergy between iron signaling and RANKL-mediated osteoclastogenesis, we propose a novel feedforward mechanism: monocytes-derived ferritin cooperates with RANKL to potentiate macrophages differentiation into hyperactive osteoclasts, thereby accelerating alveolar bone resorption. This study systematically investigates ferritin's pleiotropic roles in periodontal osteolysis through integrated clinical, murine, and *in vitro* models.

Materials and methods

Ethics statement

This study was approved by the Review Board and the Ethics Committee of Peking University Health Science Center (PKUSSIRB-2011007). All clinical specimens were obtained from patients who provided written informed consent to use their tissues for research purposes.

Sample collection

The study was approved by the Ethics Committee of Peking University Health Science Center. All clinical specimens were obtained from participants, who provided written informed consent to use their periodontal tissues for research purposes. A total of 10 participants diagnosed with periodontitis were recruited from the Department of Periodontology, Peking University Hospital of Stomatology, China. All individuals were examined to determine their periodontal status. Periodontal examination included periodontal probing depth and bleeding index using a Williams periodontal probe at six sites on each tooth. The tissue specimens were taken from patients with periodontitis who received tooth-extraction or periodontal tissue regeneration. The harvested gingival tissues were fixed in 4 % paraformaldehyde for hematoxylin and eosin (H&E) staining or 2.5 % glutaraldehyde for ultrastructural analysis.

Immunohistochemical staining of human gingival samples

After deparaffinization of samples with xylene and rehydration with ethanol, endogenous peroxidase was inactivated by incubation with 3 % H_2O_2 at room temperature for 20 min. Antigen retrieval was achieved by trypsin digestion at 37 °C for 20 min. Then, the specimens were blocked with 10 % normal goat serum at room temperature for 30 min and incubated with primary antibodies against CD68 and CD4 at 4 °C overnight. After washing three times with phosphate-buffered saline, the locations of CD68 and CD4 were visualized using an immunohistochemistry kit and a DAB detection kit (Zhongshan Golden Bridge Biotechnology, Beijing, China). Sections were finally mounted and images

were captured on a light microscope (BX51/DP72, Olympus, Tokyo, Japan).

Transmission electron microscopy (TEM)

Samples were fixed with 2.5 % glutaraldehyde and post-fixed in 1 % osmic acid, dehydrated with gradient alcohols, replaced with propylene oxide, and embedded in Epon 812. Ultrathin sections were stained with uranyl acetate and lead citrate and examined on a JEM-1400 electron microscope.

Cell culture

THP-1 cells and RAW264.7 cells were cultured in Dulbecco's modified Eagle's medium (DMEM; Gibco, Grand Island, NY, USA.) supplemented with 10 % fetal bovine serum (FBS) and 1 % penicillin and streptomycin. The cells were cultured in a humidified 5 % CO_2 atmosphere at 37 °C. RAW264.7 cells were seeded in plates (Corning, Rochester, NY, USA). THP-1 cells were induced by medium with 0, 1, 2, and 4 μg/ml *P. gingivalis*-LPS (Ultrapure lipopolysaccharide from *P. gingivalis*, TLR4 ligand, InvivoGen, Toulouse, France) for 24 h. RAW264.7 cells were induced by medium with gradient increasing apoferritin (Sigma—Aldrich, St. Louis, MO, USA) containing 0 or 25 ng/mL RANKL (Peprotech, Rocky Hill, NJ, USA). The cells were cultured for different numbers of hours.

Enzyme-linked immunosorbent assay (ELISA)

THP-1 cells were treated with *P. gingivalis*-LPS for 24 h. The culture supernatant was collected, centrifuged, and stored at −80 °C. The concentrations of ferritin and RANKL secreted by THP-1 cells were measured using ELISA kits (Telenbiotech, Chongqing, China).

Experimental animals

The study protocol was approved by the Experimental Animal Welfare Ethics Branch of Peking University Biomedical Ethics Committee (Protocol LA2013-32). Male C57BL/6 mice (8—10 weeks old) were randomly divided into groups. In the periodontitis groups ($n = 5$), a 5/0 cotton ligature was placed around the gingival margin of the second molars and left for 7 days. And the mice in the control group underwent sham operated without ligation. Mice were sacrificed 7 days later. Upper jaw samples were excised and fixed in 4 % paraformaldehyde (pH 7.4) overnight at room temperature. Then the samples were demineralized in buffered 20 % EDTA at 37 °C for 14 days, then embedded and cut on a microtome set at 5 μm. Some sections from each sample were stained with H&E and others were subjected to TRAP staining.

TRAP staining

After 3 days in culture, RAW264.7 cells were washed with 37 °C phosphate-buffered saline. Paraformaldehyde (4 %) was used to fix cells at 37 °C for 20 min. Then the cells were stained for TRAP activity (Sigma—Aldrich No. 387, St. Louis, MO, USA) at 37 °C for 1 h avoiding light. MiliQ water at 37 °C was used to wash cells. Nuclei were counterstained with hematoxylin. The coverslips were placed on glass slides. Cellular Images were captured on a microscope with a digital camera (BX51/DP72, Olympus, Tokyo, Japan). The TRAP-positive multinucleated cells were quantified in 10 visual fields chosen at random from different areas of each coverslip.

RNA extraction and real-time polymerase chain reaction (RT-PCR) analysis

Total RNA was extracted from treated RAW264.7 cells using TRIzol (Invitrogen, Carlsbad, CA, USA). Then, RNA was used for cDNA synthesis with a reverse transcription system (Toyobo, Osaka, Japan). The synthetic cDNA was mixed with power SYBR green PCR master mix (Roche, Indianapolis, IN, USA) and gene-specific primers. Real-time PCR was performed using a 7500 real-time PCR detection system (Applied Biosystems, Foster City, CA, USA). The amplification conditions consisted of an initial 10 min denaturation step at 95 °C, followed by 40 cycles of denaturation at 95 °C for 15 s, annealing at 60 °C for 60 s, and elongation at 72 °C for 30 s. The relative expression levels of targets were assessed using the comparative $2^{\Delta\Delta Ct}$ method. The primers were synthesized by Sangon Biotech (Shanghai, China) as follows: 5′-ATGGGGAAGGTGAAGGTCG-3' (forward primer) and 5′-GGGGTCATTGATGGCAACAAT-3' (reverse primer) for the mouse glyceraldehyde-3-phosphate dehydrogenase (GAPDH) gene, 5′-AAAGACCTGAAAACCTCCAAC-3' (forward primer) and 5′-GACTGCTTCTCTCCCATCATC-3' (reverse primer) for the mouse MMP-9 gene, 5′- GGCCAGTGTGGTTCCTGTTGG-3' (forward primer) and 5′-CCGCCTCCACAGCCATAATTCTC-3' (reverse primer) for the mouse CTSK gene, 5′-CAAGAACTTGCGACCATTGTTA-3' (forward primer) and 5′-ATCCATAGTGAAACCGCAAGTA-3' (reverse primer) for the mouse TRAP gene.

Statistical analysis

Statistical analyses were applied using SPSS 26.0 and GraphPad Prism 9 software. Results are presented as the mean ± standard error of the mean (SEM) using Student's t-test for paired comparisons and one-way analysis of variance (ANOVA) for testing multiple groups. A value of $P < 0.05$ was considered statistically significant.

Results

Monocyte-derived macrophages dominate inflammatory infiltrates in periodontitis

Histopathological analysis revealed striking contrasts between healthy and periodontitis-affected gingival tissues. In healthy controls, subepithelial connective tissue demonstrated well-organized collagen bundles with minimal cellular infiltration. Conversely, periodontitis specimens exhibited extensive inflammatory remodeling characterized by dense aggregates of leukocytes displacing

collagen matrix and proliferative vasculature with dilated lumens (Fig. 1A). Immunophenotyping identified $CD68^+$ immune cells exhibited a diffuse infiltration pattern, and $CD4^+$ immune cells were clustered in perivascular regions (Fig. 1B and C). Notably, macrophage density positively correlated with radiographic bone loss severity, supporting their central role in osteolytic pathogenesis. These findings establish inflamed gingiva as a reservoir of osteoclast precursors, though the precise differentiation signals within this niche remain to be elucidated.

Monocytes-derived ferritin potentiates RANKL signaling under inflammatory stimulation

The pathogenesis of vertical alveolar bone resorption in periodontitis involves coordinated interactions between microbial virulence factors and host immune cells. Mechanistically, exposure of THP-1 cells to *P. gingivalis*-LPS (0–4 μg/mL, 24 h) triggered dose-dependent secretion of both ferritin and RANKL ($P < 0.01$ vs. untreated controls; Fig. 2A and B). This synergistic induction suggests a coordinated mechanism whereby pathogen-associated molecular patterns (PAMPs) simultaneously activate iron storage and osteoclastogenic pathways. While RANKL's role in promoting osteoclast precursor fusion is well-established,[15] our findings unveil ferritin as a novel inflammatory mediator in this process. The co-secretion pattern implies that ferritin may modulate RANKL signaling potentially via redox regulation or enhancing osteoclast precursor iron bioavailability for metabolic activation.[16]

Apoferritin and RANKL synergistically drive osteoclast precursor expansion

To dissect the interplay between ferritin and RANKL in osteoclastogenesis, we quantified their combinatorial effects on RAW264.7 pre-osteoclast proliferation. Cells (8×10^4/mL) were treated with escalating apoferritin doses (0–10 μg/mL) alongside a fixed RANKL concentration (25 ng/mL), mimicking the inflammatory milieu of

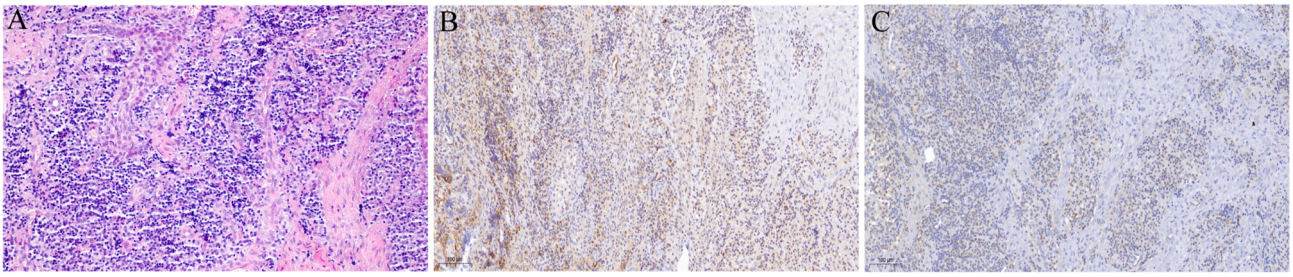

Figure 1 Inflammatory gingival tissues have a large number of infiltrating mononuclear macrophages. (A) Hematoxylin and eosin staining. The connective tissue of inflamed gingiva is rich in inflammatory cells and red blood cells, and staining for CD68 (B) and CD4 (C). The distribution range of mononuclear macrophages in inflammatory gingival tissue is consistent with that of inflammatory cells.

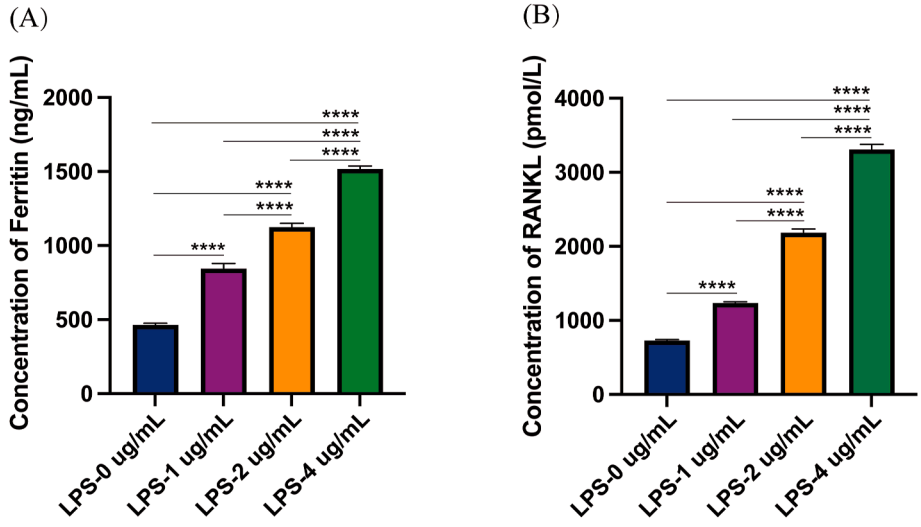

Figure 2 *P. gingivalis*-LPS induces ferritin and RANKL production in THP-1 cells. THP-1 cells are stimulated with different concentrations of *P. gingivalis*-LPS for 24 h. The protein levels of ferritin (A) and RANKL (B) from cultured supernatants are assessed by ELISA. The experiments were repeated at least three times. Results are presented at the mean ± SEM. ****$P < 0.0001$ versus untreated cells. *P. gingivalis*-LPS, *Porphyromonas gingivalis* lipopolysaccharide; RANKL, receptor activator of nuclear factor-κB ligand.

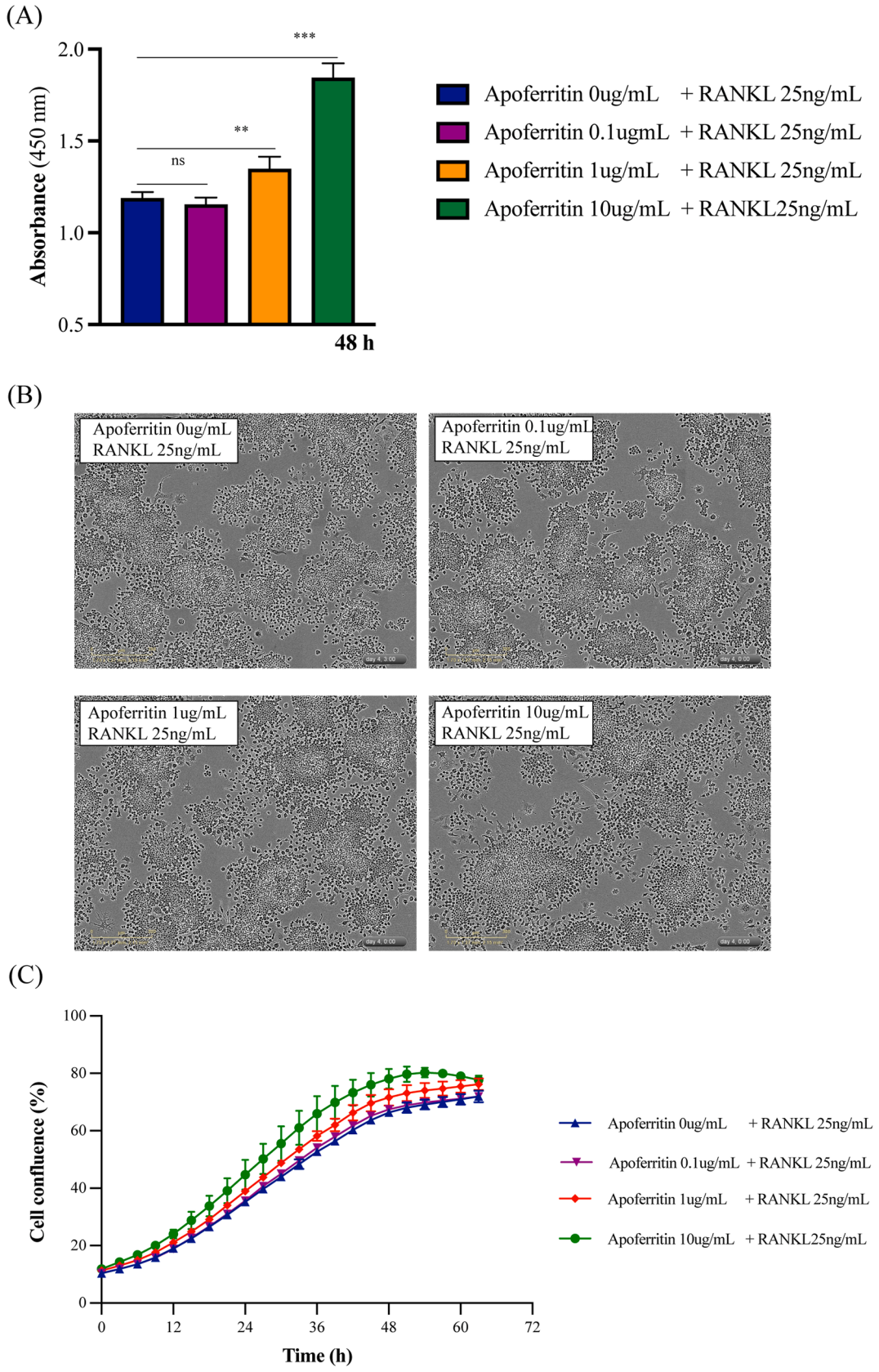

Figure 3 The synergistic effect of extracellular ferritin and RANKL promotes the proliferation of RAW264.7 cells. (A) After the cells are inoculated on 96-well plates, Cell Counting Kit-8 (CCK-8) assays are used to verify the results at 48 h. (B, C) IncuCyte is used for real-time analysis of the cell polymerization. 10 μg/mL apoferritin and RANKL have a synergistic effect, which significantly improves the proliferation of RAW264.7 cells. $^{**}P < 0.01$, $^{***}P < 0.001$ versus controls. RANKL, receptor activator of nuclear factor-κB ligand.

periodontitis. The CCK-8 results showed that a high concentration of apoferritin significantly promoted the proliferation of RAW264.7 cells (Fig. 3A). RAW264.7 cells were divided into the following experimental groups: Apoferritin 0 μg/mL + RANKL 25 ng/mL, Apoferritin 0.1 μg/mL + RANKL 25 ng/mL, Apoferritin 1 μg/mL + RANKL 25 ng/mL, and Apoferritin 10 μg/mL + RANKL 25 ng/mL. Interestingly, when the concentration of apoferritin was increased to 1 μg/mL and 10 μg/mL, the proliferation of RAW264.7 cells was significantly improved, and the synergic effect of medium–high apoferritin and RANKL significantly improved the proliferation of RAW264.7 cells. Cells were also monitored in real time using IncuCyte ZOOM® (Fig. 3B and C). When the periodontal pathogenic factors lead to the simultaneous increase of RANKL and ferritin in periodontal tissues, the proliferation of mononuclear macrophages is significantly improved.

Monocyte-macrophage fusion generates osteoclast precursors in periodontal granulation tissue

Ultrastructural analysis of infrabony granulation tissue from periodontitis patients revealed a dynamic three-phase maturation cascade driving osteoclast precursor formation (Fig. 4). Phase I-monocyte recruitment (Fig. 4A and B): circulating monocytes infiltrating through dilated capillaries exhibited activated phenotypes - enlarged nuclei, mitochondrial proliferation, and expanded rough endoplasmic reticulum (ER) networks indicating metabolic preparation for differentiation. Phase II-fusion initiation (Fig. 4C and D): adjacent macrophages engaged in membrane blebbing and pseudopod interdigitation, contacting cells showing partial organelle mixing. Phase III-functional maturation (Fig. 4E and F): emerging multinucleated giants contained more than 3 nuclei with active nucleoli, developing ruffled borders, and lysosomal density higher than mononuclear cells, demonstrating functional specialization for bone resorption. These ultrastructural features corroborate our *in vitro* findings that ferritin-RANKL signaling enhances cells fusion.

Apoferritin promotes the differentiation of RAW264.7 cells

To explore the impact of ferritin on osteoclast differentiation, RAW264.7 cells were treated with apoferritin (0–10 μg/mL) in the presence or absence of RANKL (25 ng/mL) for 5 days. TRAP staining results showed that the combination of 10 μg/mL apoferritin and RANKL significantly increased the number of TRAP-positive multinucleated cells compared to RANKL alone. Notably, 10 μg/mL apoferritin alone also induced a substantial number of

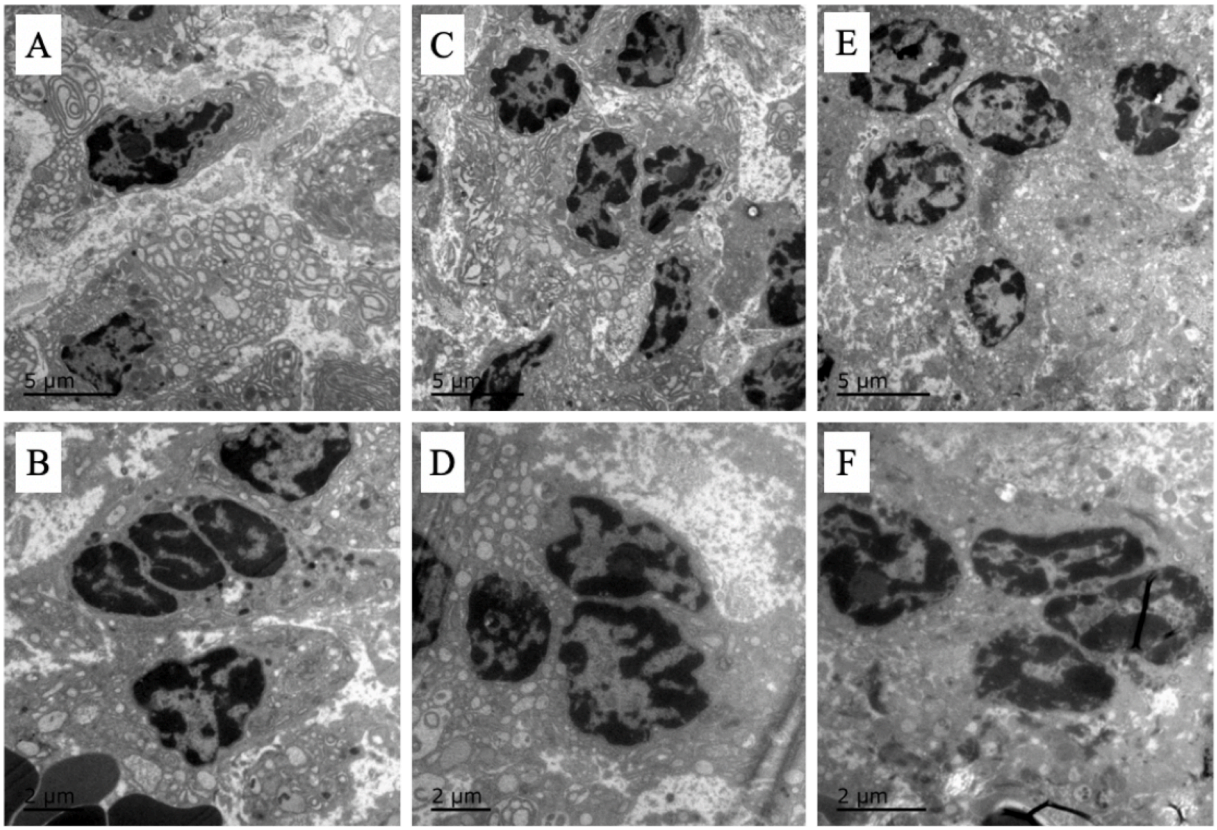

Figure 4 Osteoclast precursor maturation in periodontal granulation tissue. (A, B) Phase I: recruited monocytes near capillary with abundant mitochondria and expanded ER. (C, D) Phase II: macrophages undergoing fusion with membrane blebs and shared cytoplasm. (E, F) Phase III: mature multinucleated cell with lysosomes and vesicular trafficking systems. ER, endoplasmic reticulum.

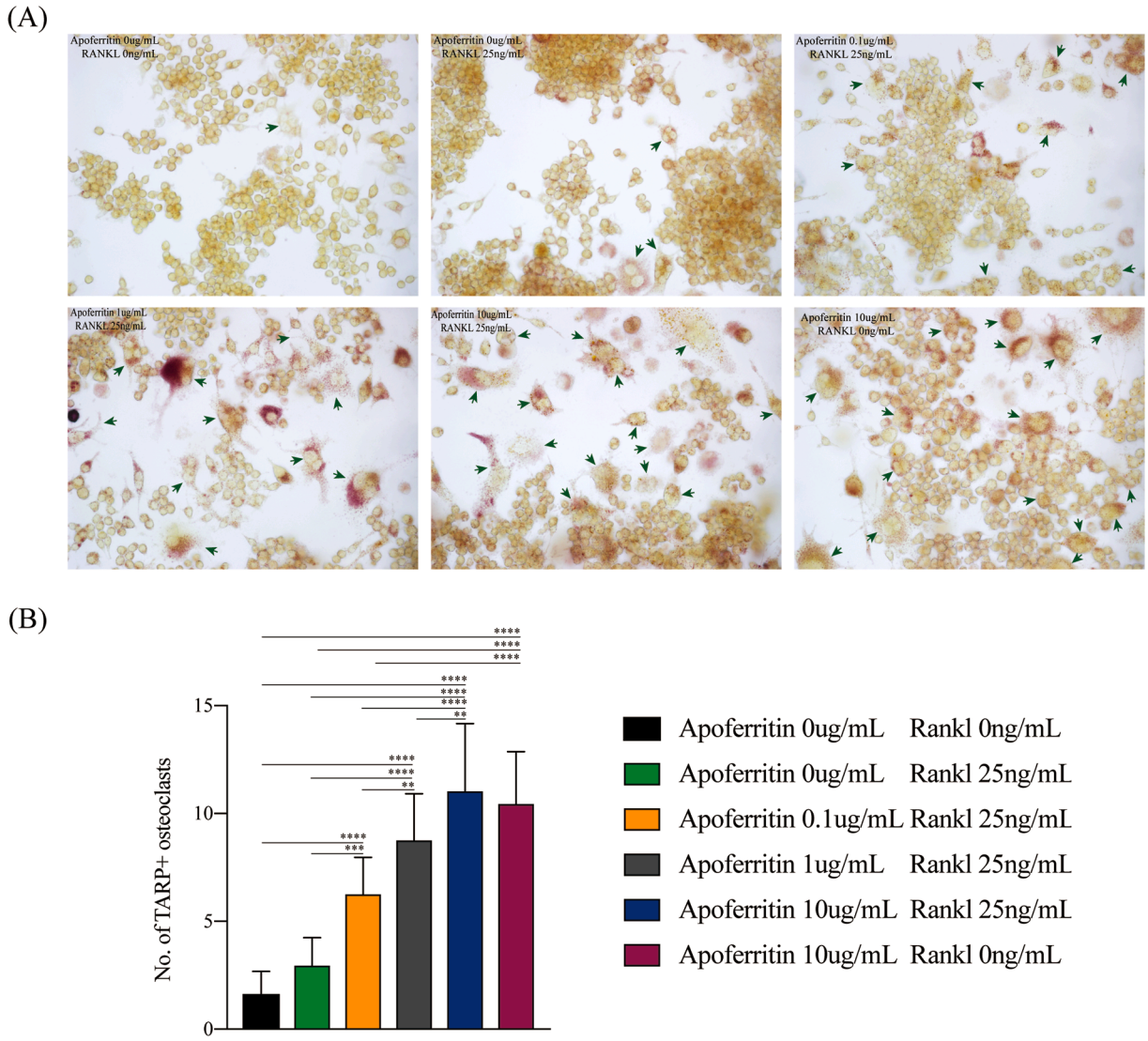

Figure 5 Ferritin synergizes with and acts independently of RANKL to drive osteoclast differentiation. (A) Representative TRAP-stained osteoclasts. (B) Quantification of $TRAP^{+}$ multinucleated (≥3 nuclei) cells/field. Mean ± SEM; *$P < 0.05$, **$P < 0.01$, ***$P < 0.001$, ****$P < 0.0001$ versus untreated cells. TRAP, tartrate-resistant acid phosphatase.

osteoclasts, exceeding the effect of RANKL alone (Fig. 5). These findings suggest ferritin activates both RANKL-dependent and iron-mediated non-canonical pathways, potentially through HIF-1α/IRP2 signaling and ROS-driven NFATc1 activation, offering new therapeutic targets for RANKL-refractory periodontitis bone loss.[17,18]

Distribution of osteoclasts in periodontal tissues of mice with experimental periodontitis

In a murine model of ligature-induced periodontitis, TRAP staining highlighted distinct differences in osteoclast distribution between healthy and diseased tissues. In control mice, the periodontal tissues exhibited intact junctional epithelium and well-organized collagen fibers, with minimal osteoclast activity indicative of normal bone remodeling (Fig. 6A and B). Conversely, in mice subjected to 7-day ligation, pathological changes were evident: loss of epithelial integrity, collagen matrix degradation, and active alveolar bone resorption. Notably, the density of osteoclasts increased significantly along the resorption lacunae (Fig. 6C and D). These spatial patterns confirm that the ferritin-mediated osteoclast activation observed *in vitro* extends to inflammatory bone loss *in vivo*, reinforcing the role of ferritin in periodontitis progression.

Ferritin-RANKL synergy upregulates osteolytic gene networks

Quantitative RT-PCR analysis demonstrated that apoferritin (0—10 μg/mL) dose-dependently enhanced RANKL-mediated transcription of osteolytic genes in RAW264.7 cells (Fig. 7). Co-stimulation with 10 μg/mL apoferritin and 25 ng/mL RANKL resulted in the highest expression levels of osteoclast-related genes. Specifically, MMP-9, CTSK, and TRAP mRNA levels were significantly

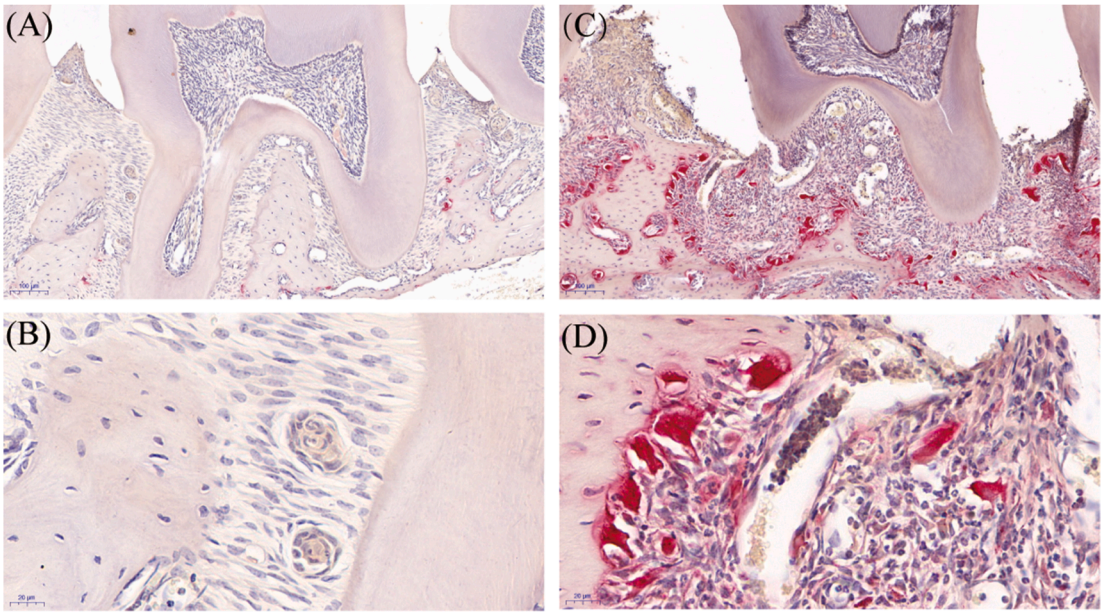

Figure 6 Pathological osteoclast expansion in experimental periodontitis. (A, B) In the healthy control group, periodontal tissues show minimal inflammatory cell infiltration and normal bone remodeling, with only a few osteoclasts (TRAP red) present. (C, D) After 7 days of experimental periodontitis ligation, dense infiltration of inflammatory cells occupies the connective tissue, and a large number of osteoclasts (TRAP red) are observed on the alveolar bone surface in the inflammatory infiltrated area. Scale bars: 100 μm (A, C) or 20 μm (B, D). TRAP, tartrate-resistant acid phosphatase.

upregulated compared to the control group. Notably, 10 μg/mL apoferritin alone also induced a substantial increase in MMP-9 and TRAP expression, exceeding the levels observed with RANKL alone. This transcriptional activation correlates with enhanced osteoclast function, as MMP-9 is involved in collagen matrix degradation, while CTSK and TRAP are key mediators of mineral dissolution. These findings highlight the synergistic effect of ferritin and RANKL in promoting osteoclastogenesis and bone resorption.

Discussion

Our study unveils a previously unrecognized axis of periodontal bone destruction, wherein monocytes-derived ferritin synergizes with RANKL to drive pathologic osteoclastogenesis. Three key discoveries emerge: (1) *P. gingivalis*-LPS triggers ferritin/RANKL co-secretion from monocytes, establishing a pro-osteolytic niche; (2) Ferritin independently activates osteoclast differentiation; (3) The ferritin-RANKL synergy amplifies bone-resorptive genes (MMP9, CTSK, TRAP). These mechanisms collectively explain the clinical correlation between elevated crevicular ferritin levels and rapid alveolar bone loss in periodontitis.[19–21] This iron-centric paradigm challenges traditional views of periodontal bone remodeling.

The periodontal microenvironment exhibits a dynamic cellular shift during disease progression. While neutrophils dominate early inflammation,[22] our research analysis revealed $CD68^+$ and $CD4^+$ immune cells constitute most of infiltrating cells in chronic lesions (Fig. 1). This aligns with single-cell RNA sequencing data showing expanded monocyte/lymphocyte clusters in periodontitis.[23]

Ferritin, an iron-binding protein, is ubiquitous and highly conserved.[14,24,25] It is an acute-phase reactant, and is elevated in chronic infection and inflammation.[26,27] Previous studies have shown that ferritin is upregulated in periodontitis and promotes inflammatory cytokine expression in human periodontal ligament cells through the transferrin receptor via the ERK/P38 pathway.[28] In this research, we found that at pathologically elevated concentrations observed in severe periodontitis, ferritin alone induces MMP9 and TRAP expression. This dual functionality enables ferritin to serve as a molecular bridge between microbial challenge and bone resorption. By integrating microbial (LPS) and metabolic (iron) cues, ferritin emerges as a master regulator of pathologic osteoclastogenesis.

Bone mass loss is regulated by the RANK-RANKL-OPG system, which is a major regulator of osteoclast differentiation, activation, and survival.[29,30] Monocytes from the blood or bone marrow of alveolar bone migrate into inflamed periodontal sites, fuse into multinuclear giant cells, and differentiate into osteoclasts under the stimulation of pathogenic periodontal bacteria, leading to alveolar bone loss. Ferritin promotes the osteoclastic differentiation of mononuclear macrophages when stimulated by periodontal pathogens as a molecular mediator. Ferritin and RANKL have a synergistic effect to significantly improve the proliferation and osteoclastic differentiation of RAW264.7 cells, as well as the expression levels of the intracellular osteoclast-related genes MMP9, CTSK, and TRAP, which may be involved in local alveolar bone resorption.

However, this study has limitations. First, the exclusive use of *P. gingivalis*-LPS *in vitro* overlooks potential contributions of other periodontal pathogens or polymicrobial interactions to ferritin modulation. Second, while THP-1

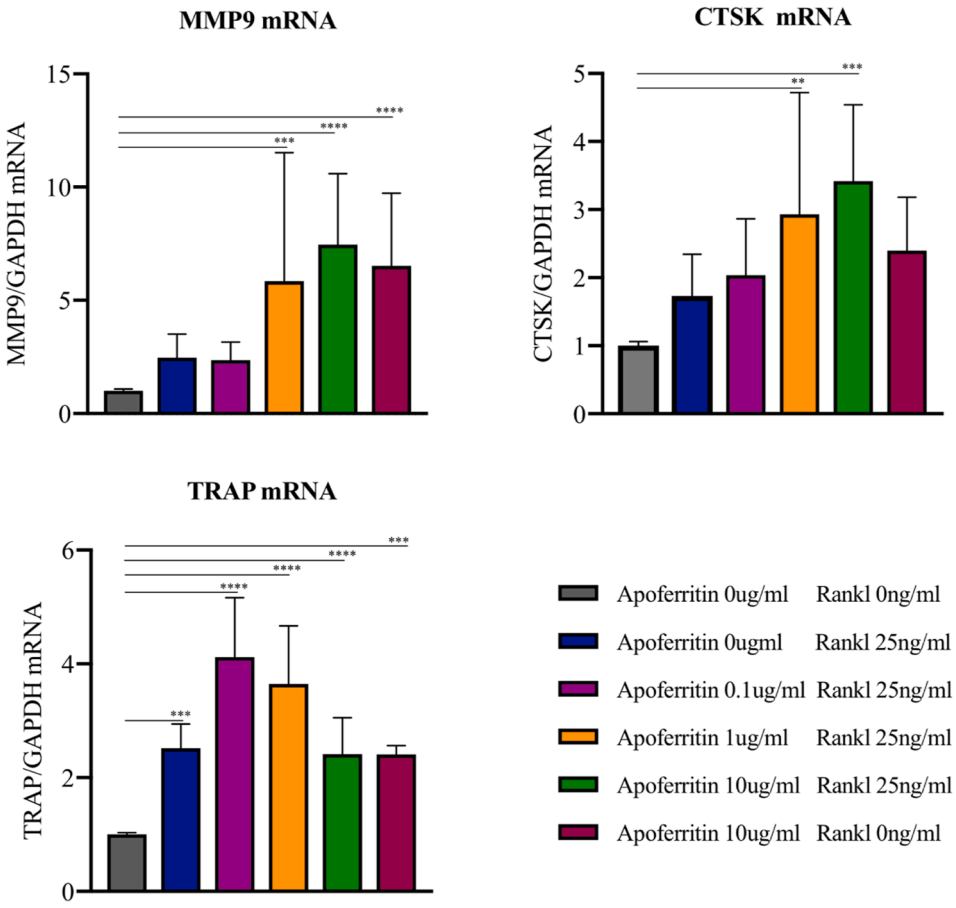

Figure 7 Ferritin coordinates osteolytic gene expression in pre-osteoclasts. Real-time PCR analysis of MMP-9, CTSK, and TRAP mRNA levels in RAW264.7 cells after 5-day treatment. RANKL alone induced modest upregulation of osteolytic genes, while the combination of high-dose apoferritin and RANKL resulted in synergistic upregulation. Apoferritin alone (10 μg/mL) also significantly activated gene expression in a RANKL-independent manner. Data are presented as mean ± SEM; $^{**}P < 0.01$, $^{***}P < 0.001$, $^{****}P < 0.0001$ vs. untreated control. PCR, polymerase chain reaction; MMP-9, matrix metallopeptidase 9; CTSK, cathepsin K; TRAP, tartrate-resistant acid phosphatase; RANKL, receptor activator of nuclear factor-κB ligand.

and RAW264.7 cells are established models, their transformed nature may not fully replicate primary monocyte/macrophage behavior in chronic inflammation. Nevertheless, by elucidating ferritin's dual role as inflammatory mediator and osteoclastogen, we redefine periodontal bone loss as a maladaptive iron signaling disorder. Therapeutic disruption of the ferritin-RANKL axis-through localized deferoxamine delivery or anti-ferritin biologics-represents a precision medicine approach to preserve alveolar architecture. Collectively, this work shifts the therapeutic focus from microbial eradication to host iron metabolism modulation, opening new avenues for periodontitis management.

Declaration of competing interest

The authors have no conflicts of interest relevant to this study.

Acknowledgements

This work was supported by the research funds from Youth Fund of Beijing Shijitan Hospital, Capital Medical University, China [grant number: 2020-q04]; Beijing Natural Science Foundation, China [grant number: 7252165].

References

1. Coll PP, Lindsay A, Meng J, et al. The prevention of infections in older adults: oral health. *J Am Geriatr Soc* 2020;68:411—6.
2. Di Benedetto A, Gigante I, Colucci S, Grano M. Periodontal disease: linking the primary inflammation to bone loss. *Clin Dev Immunol* 2013;2013:503754.
3. Cekici A, Kantarci A, Hasturk H, Van Dyke TE. Inflammatory and immune pathways in the pathogenesis of periodontal disease. *Periodontol* 2000 2014;64:57—80.
4. Yu W, Zhong L, Yao L, et al. Bone marrow adipogenic lineage precursors promote osteoclastogenesis in bone remodeling and pathologic bone loss. *J Clin Investig* 2021;131:e140214.
5. Hall-Stoodley L, Costerton JW, Stoodley P. Bacterial biofilms: from the natural environment to infectious diseases. *Nat Rev Microbiol* 2004;2:95—108.
6. Wu S, Wu B, Liu Y, Deng S, Lei L, Zhang H. Mini review therapeutic strategies targeting for biofilm and bone infections. *Front Microbiol* 2022;13:936285.
7. Stern JL, Slobedman B. Human cytomegalovirus latent infection of myeloid cells directs monocyte migration by up-

regulating monocyte chemotactic protein-1. *J Immunol* 2008; 180:6577—85.
8. Veis DJ, O'Brien CA. Osteoclasts, master sculptors of bone. *Annu Rev Pathol* 2023;18:257—81.
9. Teitelbaum SL. Bone resorption by osteoclasts. *Science* 2000; 289:1504—8.
10. Miyazaki Y, Nakayamada S, Kubo S, et al. Th22 cells promote osteoclast differentiation via production of IL-22 in rheumatoid arthritis. *Front Immunol* 2018;9:2901.
11. Lappin DF, Koulouri O, Radvar M, Hodge P, Kinane DF. Relative proportions of mononuclear cell types in periodontal lesions analyzed by immunohistochemistry. *J Clin Periodontol* 1999; 26:183—9.
12. Huang W, Li W, Liu J, Hou J, Meng H. Ferritin expression in the periodontal tissues of primates. *Eur J Histochem* 2019;63:3046.
13. Hou J, Yamada S, Kajikawa T, et al. Role of ferritin in the cytodifferentiation of periodontal ligament cells. *Biochem Biophys Res Commun* 2012;426:643—8.
14. Huang W, Zhan Y, Zheng Y, Han Y, Hu W, Hou J. Up-regulated ferritin in periodontitis promotes inflammatory cytokine expression in human periodontal ligament cells through transferrin receptor via ERK/P38 MAPK pathways. *Clin Sci (Lond)* 2019;133:135—48.
15. Dou C, Li J, Kang F, et al. Dual effect of cyanidin on RANKL-induced differentiation and fusion of osteoclasts. *J Cell Physiol* 2016;231:558—67.
16. Jiang Z, Qi G, He X, et al. Ferroptosis in osteocytes as a target for protection against postmenopausal osteoporosis. *Adv Sci (Weinh)* 2024;11:e2307388.
17. Harned J, Ferrell J, Nagar S, Goralska M, Fleisher LN, McGahan MC. Ceruloplasmin alters intracellular iron regulated proteins and pathways: Ferritin, transferrin receptor, glutamate and hypoxia-inducible factor-1alpha. *Exp Eye Res* 2012; 97:90—7.
18. Wang C, Wang G, Song F, Zhao J, Liu Q, Xu J. Antioxidant enzyme prdx1 inhibits osteoclastogenesis via suppressing ROS and NFATc1 signaling pathways. *J Cell Physiol* 2024;239: e31431.
19. Guo LN, Yang YZ, Feng YZ. Serum and salivary ferritin and hepcidin levels in patients with chronic periodontitis and type 2 diabetes mellitus. *BMC Oral Health* 2018;18:63.
20. Latha S, Thirugnanamsambandan S, Arun RT, Masthan KM, Malathi L, Rajesh E. Serum ferritin level and red blood cell parameters in healthy controls and chronic periodontitis patients. *J Pharm BioAllied Sci* 2015;7:S184—9.
21. Chakraborty S, Tewari S, Sharma RK, Narula SC. Effect of non-surgical periodontal therapy on serum ferritin levels: an interventional study. *J Periodontol* 2014;85:688—96.
22. Beertsen W, Willenborg M, Everts V, et al. Impaired phagosomal maturation in neutrophils leads to periodontitis in lysosomal-associated membrane protein-2 knockout mice. *J Immunol* 2008;180:475—82.
23. Lee H, Joo JY, Song JM, Kim HJ, Kim YH, Park HR. Immunological link between periodontitis and type 2 diabetes deciphered by single-cell RNA analysis. *Clin Transl Med* 2023;13: e1503.
24. Torti FM, Torti SV. Regulation of ferritin genes and protein. *Blood* 2002;99:3505—16.
25. Harrison PM, Arosio P. The ferritins: molecular properties, iron storage function and cellular regulation. *Biochim Biophys Acta Bioenerg* 1996;1275:161—203.
26. Zandman-Goddard G, Shoenfeld Y. Ferritin in autoimmune diseases. *Autoimmun Rev* 2007;6:457—63.
27. Wang W, Knovich MA, Coffman LG, Torti FM, Torti SV. Serum ferritin: past, present and future. *Biochim Biophys Acta* 2010; 1800:760—9.
28. Han Y, Huang W, Meng H, Zhan Y, Hou J. Pro-inflammatory cytokine interleukin-6-induced hepcidin, a key mediator of periodontitis-related anemia of inflammation. *J Periodontal Res* 2021;56:690—701.
29. Udagawa N, Koide M, Nakamura M, et al. Osteoclast differentiation by RANKL and OPG signaling pathways. *J Bone Miner Metabol* 2021;39:19—26.
30. Wang Z, McCauley LK. Osteoclasts and odontoclasts: signaling pathways to development and disease. *Oral Dis* 2011;17: 129—42.